Journal of Photochemistry and Photobiology A: Chemistry 202 (2009) 86–91

Contents lists available at ScienceDirect

Journal of Photochemistry and Photobiology A: Chemistry

journal homepage: www.elsevier.com/locate/jphotochem

# Study of Indigo carmine as radical probe in photocatalysis

Haidong Liao*, David Stenman, Mats Jonsson

*KTH Chemical Science and Engineering, NuclearChemistry, Royal Institute of Technology, SE-100 44 Stockholm, Sweden*

ARTICLE INFO

*Article history:*
Received 27 June 2008
Received in revised form 17 October 2008
Accepted 6 November 2008
Available online 25 November 2008

*Keywords:*
Indigo carmine
Photocatalysis
Gamma radiolysis
Hydroxyl radical

ABSTRACT

The feasibility of using Indigo carmine (IC) as a probe of free radical production in photocatalysis was elucidated by comparative studies of its bleaching by γ radiolysis and $TiO_2$ photocatalysis. The γ radiation result from pH 3 to 10 shows that both •OH and $HO_2$• can bleach IC and that the bleaching yields of •OH is pH independent at ~0.7 molecules per •OH. The quantum yields ($\phi$) of •OH from Degussa p25 $TiO_2$ photocatalysis from pH 3 to 10 was determined. It was found that $\phi$ was about 4% at pH 10 and dropped to below 1% at pH 3. This agrees well with the result of photocatalysis of Fricke dosimetry at pH 1. The effects of some common inorganic anions that may affect photocatalytic systems in technical applications ($Cl^-$, $SO_4^{2-}$, $Br^-$, $HPO_4^{2-}$, $B_4O_7^{2-}$, $HCO_3^-/CO_3^{2-}$) was also investigated, showing that these ions does not inhibit the photocatalytic bleaching efficiency of IC.



## 1. Introduction

Purification and sterilization of environmental waste by titanium dioxide ($TiO_2$) photocatalysis has gained increasing attention due to its biological and chemical inertness and strong oxidizing power [1–7]. Large-scale applications of photocatalytic oxidation have recently emerged [8,9]. Some examples of such applications are: ballast water treatment onboard ships, disinfection of irrigation waters to protect against the spread of water transmitted disease and the protection of potable water for human consumption.

For photocatalysis in water, it is commonly accepted that •OH is the key reactant responsible for further oxidation of organic substrates [13–18]. Knowledge of the yield of the •OH and the factors affecting this yield is essential for comparison of photocatalytic activities of different $TiO_2$ photocatalysts. Several research groups have proposed a number of methods to measure the photocatalytic •OH formation rate, including hydrogen abstraction of methanol [13,15,16], hydroxylation of aromatic structures [17], and electron paramagnetic resonance detection by spin traps that scavenge •OH [18]. However, the above methods are relatively complicated and inconvenient for real applications.

Organic dye bleaching provides a relatively simple method for assessing photocatalytic activity by monitoring UV–vis absorbance. In the present study we have investigated the potential of Indigo carmine (IC, 5,5′-indigodisulfonic acid disodium salt, an organic dye) as a probe for quantification of photocatalytic efficiency in aqueous solution. The use of this readily available and moderately stable organic dye enables studies both in the small scale in the laboratory and on larger scale for reaction engineering of technical photocatalytic systems.

Successful attempts at applying radiation chemical knowledge on photocatalysis have been demonstrated [10–13]. The similarity between aqueous radiolysis and photocatalysis and the well known product yields in radiolysis enables us to perform a quantitative assessment of the photocatalytic yield.

In addition to the reaction with •OH, it has been reported that superoxide can bleach IC [21]. If the $HO_2$•/$O_2$•$^-$ pair can bleach IC, the pH dependence of IC bleaching in the natural water pH range of interest since we expect a reactivity difference between these radicals due to the large difference in one-electron reduction potential ($HO_2$• 1420 mV, $O_2$•$^-$ −330 mV [22]).

In this work we have performed γ radiolysis experiments from pH 3 to 10 in both air saturated and $N_2O/O_2$ saturated solutions containing IC as a reference for the photocatalysis studies performed in the same pH range. In $N_2O$ saturated solutions the hydrated electrons are converted to hydroxyl radicals while hydrogen atoms are unaffected. The different ratios of $HO_2$• to $O_2$•$^-$ in the pH range and the different yields of •OH and $HO_2$•/$O_2$•$^-$ pairs in the air and $N_2O/O_2$ saturation cases enable us to systematically study the bleaching yield of IC by •OH and superoxide, respectively.

The importance of other reactions which produce secondary radical species has also been considered. Some examples are the reactivity of pH buffers and common anions ($CO_3^{2-}$, $Br^-$, $Cl^-$, $SO_4^{2-}$) frequently present in natural waters. The effects of these anions on the decomposition of IC under gamma radiolysis and $TiO_2$ photocatalysis were investigated. The results are used to discuss the mechanism of photocatalysis.

* Corresponding author. Tel.: +46 8 52272244; fax: +46 8 7908772.
*E-mail address:* haidongliao@gmail.com (H. Liao).

1010-6030/$ – see front matter © 2008 Elsevier B.V. All rights reserved.
doi:10.1016/j.jphotochem.2008.11.008

## 2. Experimental

### 2.1. Chemicals

All chemicals used throughout this work were of analytical grade or higher and were used as received from commercial sources (Aldrich, Sigma, Degussa). Millipore Milli-Q filtered water was used throughout the experiments. The $TiO_2$ powder used was Degussa P25 with a specific surface area of $50 \pm 15\ m^2\ g^{-1}$ (BET) and mean particle size of 20 nm according to the manufacturer. However, the measured diameter of formed aggregates in Millipore water was 500 nm by Brookhaven 90Plus laser scattering particle size analyzer.

### 2.2. Gamma radiolysis experiments

Gamma radiolysis experiments were performed using a Cesium-137 source (Gammacell 1000 Elite). All irradiations were performed on 100 ml solutions using the same vessel throughout. The dose rate was determined using Fricke dosimetry. The experiments performed under $N_2O/O_2$ atmosphere (80%/20%) were bubbled for 10 min prior to radiolysis.

### 2.3. Fricke dosimetry

The Fricke dosimeter used consisted of 1 mM of $Fe(NH_4)_2(SO_4)_2$, 1 mM NaCl, 400 mM of $H_2SO_4$, the formation of ferric ions was measured at 304 nm, $\varepsilon_{(Fe3+,\ 304nm)} = 2174\ cm^{-1}\ M^{-1}$ was determined experimentally. The rate of $Fe^{3+}$ formation was determined by calculating the slope of the linear curve obtained by plotting the $Fe^{3+}$ concentration as a function of time.

### 2.4. Photocatalytic experimental setup

All photocatalytic experiments were performed under irradiation from two black light lamps (15 W, Phillips Blacklite). The wavelength range and peak wavelength were determined (Hamamatsu PMA-12 spectrometer) to 345–385 and 365 nm, respectively, with an average intensity of $0.1\ mW\ cm^{-2}$, at the irradiation distance. All samples to be irradiated were placed in a blackened Petri dish (glass) of 9.0 cm inner diameter, at a volume of 40 ml. The samples were stirred by a magnetic stirrer to obtain a homogenous mixing of the suspension. The decomposition rate of Indigo carmine was determined by calculating the slope of the linear curve obtained by plotting the concentration as a function of time.

### 2.5. Analysis

All samples containing titanium dioxide were filtered through 0.2 μm membrane filters (Whatman) or centrifuged prior to further analysis. The decomposition of Indigo carmine was subsequently monitored by spectrophotometer (JASCO V-630) at 610 nm with extinction coefficient $19375\ cm^{-1}\ M^{-1}$. pH of solutions and suspensions was determined by Metrohm 713 pH meter under stirring.

## 3. Results and discussion

### 3.1. Gamma radiolysis

The primary γ radiolysis products of water are listed in reaction (1):

$$H_2O \xrightarrow{\gamma} e_{aq}^-,\ {}^\bullet H,\ {}^\bullet OH,\ H_2O_2,\ H_2 \quad (1)$$

Although reaction between Indigo carmine and the hydrated electron is diffusion controlled as reported in [19]. In aerated dilute solution of IC, the highly reactive solvated electron and hydrogen atom will primarily react with the dissolved oxygen, present in much higher concentration than that of IC, resulting in the formation of $HO_2^\bullet/O_2^{\bullet-}$ with p*K*a 4.8 ([20], p. 278).

$$^\bullet H + O_2 \rightarrow HO_2^\bullet \quad (2)$$

$$e_{aq}^- + O_2 \rightarrow O_2^{\bullet-} \quad (3)$$

Combining the *G*-values ([20], p. 260) with the determined dose rates by Fricke dosimetry, the production rates of $^\bullet OH$ and $HO_2^\bullet/O_2^{\bullet-}$ are calculated to $2.7\ \mu M\ min^{-1}$ and $3.3\ \mu M\ min^{-1}$, respectively, in air saturated solution, and $5.4\ \mu M\ min^{-1}$ and $0.6\ \mu M\ min^{-1}$, respectively, in $N_2O/O_2$ saturated solution.

Bleaching of Indigo carmine was studied as a function of pH to elucidate the reactivity of IC towards $^\bullet OH$ and $HO_2^\bullet/O_2^{\bullet-}$ in the chemical systems described above (in air and $N_2O/O_2$ saturated aqueous solutions). 1 mM phosphate buffers were used to adjust the pH to 6, 7 and 8. Perchloric acid ($HClO_4$) and sodium hydroxide (NaOH) were used to adjust the initial pH to 3, 4, 5 and 9, 10 respectively.

The experiments were performed in duplicates. A typical IC concentration versus irradiation time plot is shown in Fig. 1. The decomposition rates as a function of pH for air and $N_2O/O_2$ saturated solutions are plotted in Fig. 2.

From the results presented in Fig. 2, it can be seen that the bleaching yield of IC (G(-IC)) under $N_2O/O_2$ is constant over the pH-range 3–10. This shows that the bleaching of IC by $^\bullet OH$ is independent of pH. Moreover, G(-IC) under air saturation at alkaline pH is precisely half of that measured under $N_2O/O_2$ and the decreasing G(-IC) observed with increasing pH for air saturated solutions reveals that $HO_2^\bullet$ is indeed capable of bleaching IC. This is further evidenced by the fact that, under acidic conditions, the G(-IC) increases under air saturation to reach the same level as that observed for $N_2O/O_2$. From the data presented it may be

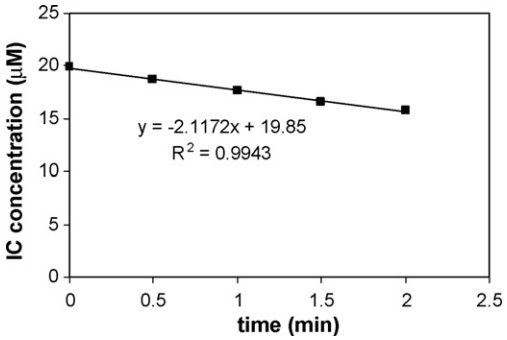


**Fig. 1.** Concentration of Indigo carmine measured at 610 nm plotted against the irradiation time, Initial IC concentration 20 μM, pH 9.

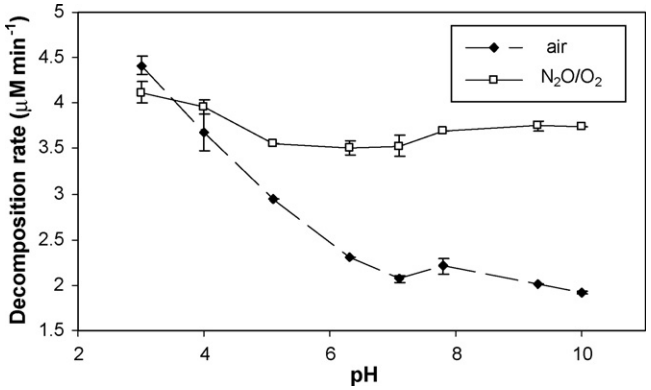


**Fig. 2.** IC decomposition rate in air and $N_2O/O_2$ saturated solutions as a function of pH.

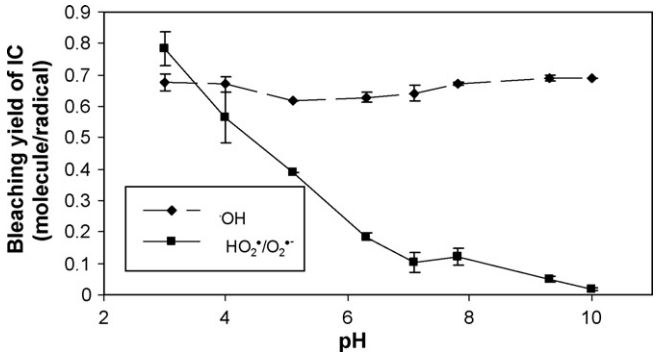


**Fig. 3.** The bleaching yield with error bar calculated from the trend of the double samples.

concluded that the majority bleaching of IC by superoxide comes from its protonated form, as suggested by Kettle et al. [21] in their two step proton driven decomposition route of Indigo carmine by superoxide at neutral pH.

Assuming the radical bleaching yields are the same in air and in $NO_2/O_2$ saturated solutions, the bleaching yield of •OH can be deduced from the IC consumption under air and $N_2O/O_2$ saturated solutions. The deduced bleaching yield by •OH is constant and was determined to be 0.7 IC molecules per •OH. The bleaching yield by $HO_2•/O_2^-$ as a function of pH is presented in Fig. 3. These values can be used in the quantum efficiency calculations in photocatalysis using IC as a chemical probe, since the radical production ration is identical to γ-radiolysis.

The fraction of superoxide in the $HO_2•/O_2•^-$ pair is higher than 99% at pH 7 and 8 (p*K*a = 4.8). The small contribution to the IC decomposition from other sources than •OH in this range can be explained by the fast equilibration of $O_2•^-$ and $HO_2•$ due to the diffusion controlled reaction of $O_2•^-$ with the proton [22], and a relatively long lifetime of superoxide. During steady state conditions, the consumed $HO_2•$ in the reaction with IC is rapidly replaced by new radicals formed upon protonation of $O_2•^-$.

Above pH 9, almost all the bleaching can be attributed to •OH. Hence, IC can be considered as a pure OH radical probe above pH 9 if no other scavengers are present. To trap all the •OH, the concentration of probe molecules should be high enough to compete with other reactions consuming •OH. Bleaching experiments at pH 10 with initial IC concentration in the range of 10–50 μM were performed. The pH was adjusted by NaOH. Results show that above 30 μM, the bleaching yield is constant at about 0.76 molecules per •OH (Fig. 4), representing the maximum net yield of •OH.

### *3.1.1. Effect of inorganic anions on bleaching of IC by gamma radiolysis*

It is well established that one-electron oxidants, such as a reactive hole or radicals in solution such as •OH, can react with dissolved

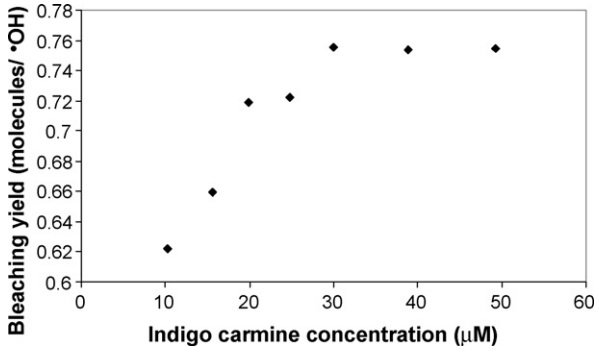


**Fig. 4.** Bleaching yield of IC versus concentrations in air saturated solutions at pH 10.

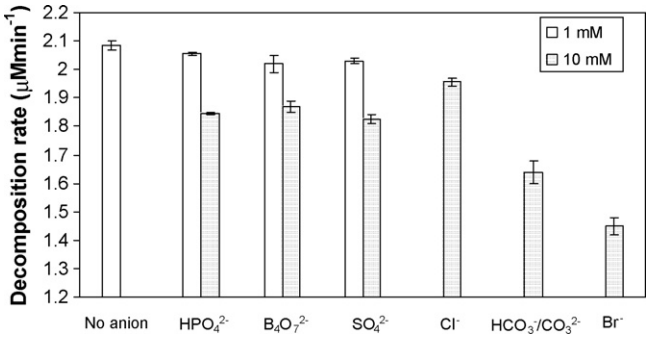


**Fig. 5.** Inorganic anion's effect in gamma radiolysis, IC concentration 50 μM, pH 10.

anions forming the corresponding radicals. There are many studies on the effects of various anions and cations on photocatalysis in aqueous solutions in the literature [23–26]. However, most of these studies have not considered the effects of dissolved anions on the radical chemistry, and its implications on the chemical systems used.

For the investigation of IC as a probe of free radical production in photocatalytic systems it is of importance to determine how various anions affect the chemical yields. Therefore, the effects of phosphate and borate buffers and some inorganic anions that are common in natural waters were investigated. The effects of $KH_2PO_4$, $Na_2B_4O_7$, NaCl, $Na_2SO_4$, $NaHCO_3$ and NaBr on IC bleaching upon γ-radiolysis at pH 10 are shown in Fig. 5. Solution equilibrium was achieved by stirring for half an hour prior to the experiments, the initial pH of the samples was adjusted by NaOH. All experiments were performed in duplicates.

The rate constants for the reaction between the studied anions and •OH, as well as the one-electron reduction potential of the radicals formed upon one-electron oxidation of the anions are shown in Table 1.

From the data presented in Table 1 we can conclude that the only radicals expected to be formed in the reaction between •OH and the corresponding inorganic salts are $Cl_2•^-$, $CO_3•^-$, $Br_2•^-$. These radicals all have the thermodynamical ability to oxidize Indigo carmine. The experimental results show that anions suppress the yield of IC bleaching in the order: $Br^- > CO_3^{2-} > B_4O_7^{2-} \approx SO_4^{2-} \approx HPO_4^{2-} > Cl^-$. Under the present experimental conditions •OH is not able to oxidize phosphate, borate and sulfate ions for both thermodynamical and kinetic reasons. The inhibiting effect (∼10%) of phosphate, borate and sulfate ions at 10 mM concentration may be due to the reduction of dissolved oxygen in high concentrated salt solution. The beneficial effect of higher dissolved oxygen concentration on the bleaching of IC in gamma radiolysis has been verified in our study.

The mechanisms of the reactions between the halide ions chloride and bromide and the •OH under alkaline conditions differ from each other [28,29]. Chloride will form chlorine-hydroxyl radical anion ($ClOH^-$) upon reaction with •OH, but it only efficiently transforms into di-chlorine radical anion under acidic conditions. Lack of $H^+$ will make the chlorine-hydroxyl radical anion transform back into the •OH and chloride, effectively extending the lifetime of the •OH. The reaction of bromide proceeds by an initial one-electron transfer reaction forming Br•. If there is sufficient $Br^-$ in solution, Br• rapidly captures a $Br^-$ to form the dibromidyl radical anion, $Br_2•^-$. Since these reactions do not involve protons, the conversion of •OH to dibromidyl is less pH dependent than that for the chloride reactions, and the yields of conversion are higher ([20], p. 302).

The conversion of OH-radicals into carbonate radicals proceeds through a one-electron transfer reaction with carbonate or hydrogen abstraction with bicarbonate. The rate constants for the reactions with $HCO_3^-$ and $CO_3^{2-}$ differ. Hence, the reaction is pH

**Table 1**
Rate constants for the reaction between •OH and inorganic ions and one-electron reduction potentials of the corresponding radicals.

| Ions | Reaction rate constant ($M^{-1}\,s^{-1}$) | Formed radical | Reduction potential (mV) | Reference |
|---|---|---|---|---|
| IC | $1.8 \times 10^{10}$ | | | [22] |
| $HPO_4^{2-}$ | $1.5 \times 10^{5}$ | | | [22] |
| $B_4O_7^{2-}$ | $\leq 1 \times 10^{6}$ | | | [22] |
| $Cl^-$ | $3 \times 10^{9}$ | $Cl_2^{\bullet-}$ | 2200 | [22] |
| $SO_4^{2-}$ | – | $SO_4^{\bullet-}$ | 2430 | [22] |
| $HCO_3^-$ | $8.5 \times 10^{6}$ | $CO_3^{\bullet-}$ | ~1600 | [22], [27] |
| $CO_3^{2-}$ | $3.9 \times 10^{8}$ | $CO_3^{\bullet-}$ | | [22] |
| $Br^{-1}$ | $1.1 \times 10^{10}$ | $Br_2^{\bullet-}$ | ~1650 | [22] |

dependent controlled by the p*K*a of carbonate at 10.3. At pH 10 about one half of carbonate ion is $CO_3^{2-}$. Using the rate constants shown in Table 1, it was determined that about 2/3 of the •OH radicals will be converted to carbonate radical anions, and the remainder will react directly with IC.

From the results shown in Fig. 5 it can be concluded that the one-electron oxidants di-bromidyl and carbonate radical anions, are less effective in bleaching Indigo carmine than the hydroxyl radical. The formation of chlorine-hydroxyl radical anion or di-chloridyl radicals by the presence of $Cl^-$ in the reaction system, does not affect the bleaching yields to any greater extent, under the conditions investigated.

### 3.2. Photocatalysis of Indigo carmine in $TiO_2$-suspension

Photocatalytic processes are initiated by absorption of UV photons with energy higher than the band gap of the photocatalyst. Conduction band electrons and valence band holes are formed according reaction (4). The electrons and holes thus produced diffuse to the surface and during this process most of them recombine again. When electron scavengers such as oxygen are present, the electrons are trapped according reaction (6), and the holes will rapidly be converted to hydroxyl radicals upon oxidation of surface water, according to reaction (7).

$$TiO_2 + h\nu \rightarrow e_{cb}^- + h_{vb}^+ \quad (4)$$

$$h_{vb}^+ + e_{cb}^- \rightarrow TiO_2 \quad (5)$$

$$e_{cb}^- + O_2 \rightarrow O_2^{\bullet-} \quad (6)$$

$$h_{vb}^+ + H_2O \rightarrow {}^{\bullet}OH + H^+ \quad (7)$$

To enable comparisons between the results obtained from the gamma radiolysis studies and a photocatalytic reaction system, a series of photocatalytic studies under varied conditions, were performed.

#### 3.2.1. Dark adsorption of Indigo carmine on $TiO_2$

There has been a multitude of studies on the effects of adsorption of substrate on the photocatalyst in different photocatalytic reaction systems [30–33]. Due to the short life time of reactive holes and free radicals, the adsorption will favor the interaction of the substrate with these radicals. The adsorption of indigo on $TiO_2$ at various pH was evaluated under $TiO_2$ loading 400 ppm and initial IC concentration 50 μM. The adsorption equilibrium of suspension was achieved in dark after one hour mixing. The percentage absorption is defined as $(C_i - C_{eq})/C_i{}^*100\%$, which $C_i$ and $C_{eq}$ is initial and equilibrium concentration, respectively. The pH was adjusted by $HClO_4$ and NaOH.

The results show that Indigo carmine is absorbed strongly at pH below the point of zero charge of $TiO_2$ ($pH_0$), previously determined at $pH_0 = 6.3$ [32,34]. At pH higher than 6.3, the absorption of IC is very small, due to the anionic nature of Indigo carmine as shown in Fig. 6.

It is well documented that when the particle of $TiO_2$ is in contact with water both dissociated and molecular water are bound

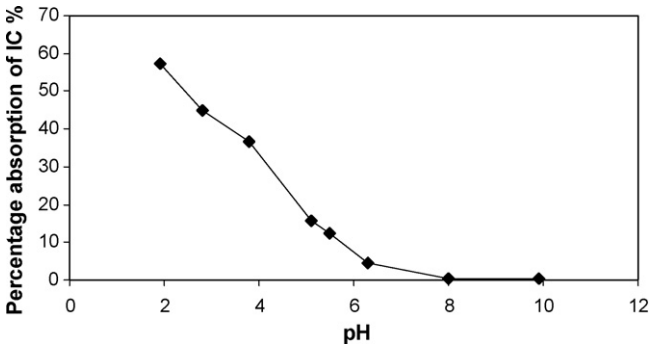


**Fig. 6.** Percentage adsorption of IC on $TiO_2$ at various of pH, initial concentration of IC = 50 μM, $TiO_2$ concentration = 400 ppm.

to the surface depending on which crystal plane is being considered [35–37]. Most researchers report the density of $OH^-$ on $TiO_2$ surface is between 7 and 10 molecules $nm^{-2}$ at room temperature [38–41]. Taking the BET value of Degussa P25, the surface density of absorbed Indigo carmine at pH 2 is 0.9 molecules $nm^{-2}$. The relative surface coverage of IC to $H_2O$ is about 10% at low pH level.

The low tendency of Indigo carmine to adsorb on $TiO_2$, under neutral and alkaline conditions, implies that most of the chemical change of the systems at neutral and alkaline conditions occurs in the aqueous phase. The diffused •OH in bulk solution should be responsible for the bleaching at these conditions, since the contribution from $O_2^{\bullet-}$ is small.

#### 3.2.2. Titanium dioxide concentration dependence

The sensitivity of Indigo carmine as a chemical probe in photocatalysis was checked by measuring the yields of indigo-bleaching at varied amounts of added photocatalyst in buffered solutions. The results are shown in Fig. 7.

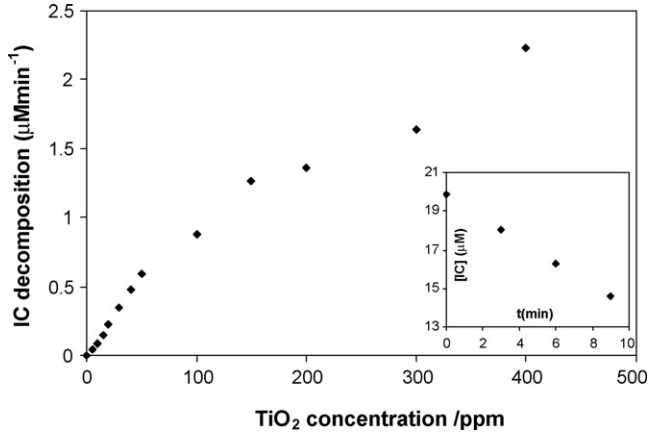


**Fig. 7.** Indigo carmine bleaching rate plotted against photocatalyst concentration in buffered (pH 7 phosphate 1 mM) aqueous solutions. Initial concentration of IC = 20 μM.

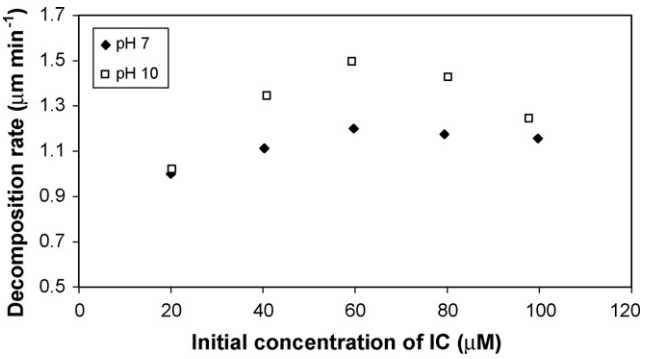


**Fig. 8.** Concentration effect of IC on photocatalysis, $TiO_2$ concentration 100 ppm.

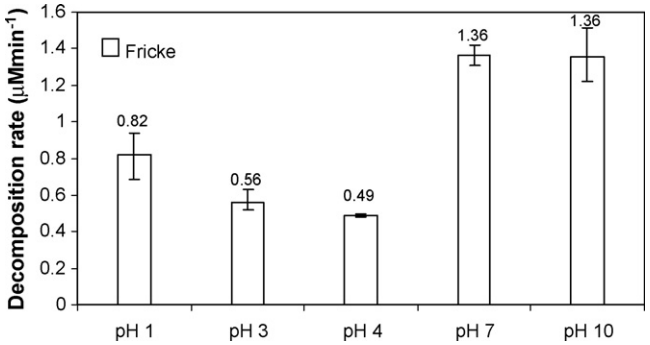


**Fig. 9.** pH effect on the photocatalytic decomposition of initial 50 μM IC and the formation of $Fe^{3+}$ during Fricke dosimetry in 100 ppm $TiO_2$-suspension.

Linear proportionality of the photocatalytic efficiency to the square root of the illumination intensity is observed by many studies [15,16,42–44]. Our results agree well with this observation. At high $TiO_2$ concentration, the light intensity on $TiO_2$ surface will be inversely proportional to the $TiO_2$ concentration. Hence, the decomposition rate at high $TiO_2$ concentration is proportional to the square root of the concentration of $TiO_2$.

### 3.2.3. Effect of concentration

From the gamma radiolysis experiments we found that the OH radical is the main oxidizing radical in the bleaching of Indigo carmine under alkaline conditions. The influence of Indigo carmine concentration on the trapping of photocatalytically produced OH radicals was studied at pH 7 and pH 10. Bleaching of IC in the concentration range 20–100 μM at 100 ppm $TiO_2$ is shown in Fig. 8. 1 mM phosphate buffer was used to adjust pH to 7, and NaOH was used to adjust pH to 10.

The results give a maximum efficiency around 60 μM, and then drop at higher concentration. This may be explained by the absorption of UV light by IC, thus reducing the portion absorbed by the $TiO_2$-particles (absorbance of 100 μM IC at 365 nm is 0.42, 100 ppm Degussa is 1.98). In all subsequent tests the IC concentration was chosen at 50 μM.

### 3.2.4. Effect of pH

In order to determine the quantum efficiency for a relevant pH range, we have performed experiments at pH 4, 7 and 10, all of which are relevant for natural waters. The results show a different trend compared to that obtained for IC bleaching during gamma radiolysis. Therefore, photocatalysis of IC at pH 3 and photocatalysis of Fricke solutions were also conducted.

The concentration of $TiO_2$ was 100 ppm, 1 mM phosphate buffer was used (pH 7), $HClO_4$ and NaOH were used to adjust the initial pH to 3, 4 and 10. The Fricke dosimetry suspensions consisted of 50 mM $H_2SO_4$, 1 mM NaCl, 1 mM $Fe(NH_4)_2(SO_4)_2$ and 100 ppm $TiO_2$. All tests were repeated four times.

The chemical reactions occurring during Fricke dosimetry is ([20], p. 288):

$$O_2^{\bullet -} + H^+ \rightarrow HO_2^{\bullet} \quad (8)$$

$$^{\bullet}OH + Fe^{2+} \rightarrow OH^- + Fe^{3+} \quad (9)$$

$$HO_2^{\bullet} + Fe^{2+} \rightarrow HO_2^- + Fe^{3+} \quad (10)$$

$$HO_2^- + H^+ \rightarrow H_2O_2 \quad (11)$$

$$H_2O_2 + Fe^{2+} \rightarrow OH^- + Fe^{3+} + {}^{\bullet}OH \quad (12)$$

From the reactions above, it is evident that one photocatalytic conversion (resulting in one $^{\bullet}OH$ from the hole and one $O_2^{\bullet -}$ from the electron) corresponds to the formation of four ferric ions.

The effect of pH on IC bleaching in photocatalysis, and the formation rate of $Fe^{3+}$ are shown in Fig. 9.

The results show two different regions of efficiency, the higher efficiency region at pH above 6 and lower efficiency region at pH below 6. Comparing the results to the observed pH effect in γ radiolysis (Fig. 2), it becomes obvious that the free radical production in photocatalysis of $TiO_2$ is significantly reduced at pH below the point of zero charge, and the direct oxidation of Indigo carmine by hole is not significant.

### 3.2.5. Effect of inorganic anions

The effect of various anions on photocatalysis was tested by adding different inorganic anions (10 mM) to a $TiO_2$-suspension (100 ppm) in the presence of IC (50 μM). The solutions were equilibrated by stirring in the dark for more than 10 h, prior to the experiments. All tests were repeated four times. The initial pH of the samples was adjusted to 10 by NaOH. The results of the experiments are presented in Fig. 10.

The results clearly show that none of the anions inhibit IC bleaching. Interestingly, the addition of carbonate and bromide enhances the bleaching yields. Comparing these results to those obtained upon addition of bromide and carbonate ions in the gamma radiolysis experiments (Fig. 5), where the bleaching yields are decreased, the only explanation for the increase in yields observed in photocatalysis is that formation of $Br_2^{\bullet -}$ and $CO_3^{\bullet -}$ by the direct oxidation by the positive hole is much more efficient than the formation of the hydroxyl radical.

Considering the lower bleaching efficiency of these radical anions (determined by gamma radiolysis), the radical production increase by photocatalysis is estimated to approximately 300% compared to that of the hydroxyl radical. This is probably due to a higher production efficiency of these radicals owing to the lower reduction potentials of the radicals formed upon oxidation of these anions.

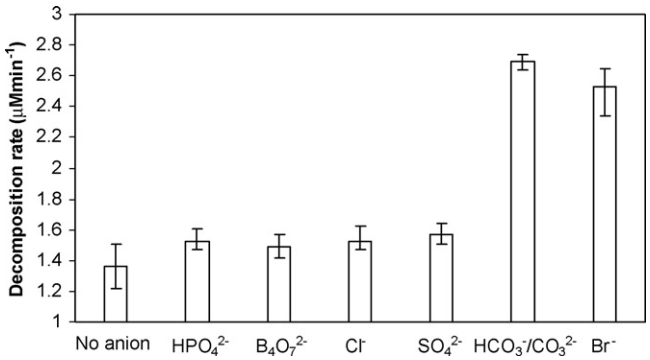


**Fig. 10.** Effect of inorganic anions on photocatalytical bleaching of IC in suspensions containing 100 ppm $TiO_2$ and 50 μM IC at pH 10.

*3.2.6. Photocatalytic quantum efficiency of OH radical*

Combining the IC bleaching yield, solution volume, photon flux and the true absorbance of Degussa p25 at 365 nm ($0.6 \times 10^4\ g^{-1}\ cm^2$)[16,45], the quantum efficiency of OH radical was calculated. The resulting quantum efficiency is 4.2% at pH 10. This value is similar to previously published values [15,16,45].

## 4. Conclusions

In this study, the method of using Indigo carmine as radical probe in photocatalytic systems was developed and investigated. The experimental results show that both hydroxyl and hydroperoxyl radical can cause bleaching of Indigo carmine, whereas the superoxide radical anion does not show any significant reactivity towards Indigo carmine. The former is pH independent and the yield ratio of •OH to IC bleaching is about 1.3. Secondary radicals formed by side reactions with other components in solution (such as bromide and carbonate) will affect the yields of oxidation. Especially attention must be paid when these ions exists in samples.

The quantum yields of OH radicals formed by photocatalysis, as determined by IC-probing, confirms the validation of this method. The methodology used in this study (parallel studies using gamma and photocatalysis) of evaluating probes for assessment of photocatalytic systems may be applied to any chemical probe of free radicals. Advantageous for this approach is the well defined radical chemistry afforded by the radiolysis methods.

## Acknowledgements

We gratefully acknowledge Wallenius Water AB, Stockholm, for financial support.

## References

[1] H.K. Yukiko, S. Yuko, K. Kunio, Chemosphere 62 (2006) 149–154.
[2] P.A. Pekakis, N.P. Xekoukoulotakis, D. Mantzavinos, Water Res. 40 (2006) 1276–1286.
[3] B. Toepfer, A. Gora, G.L. Puma, Appl. Catal. B: Environ. 68 (2006) 171–180.
[4] M.G. Antoniou, D.D. Dionysiou, Catal. Today 124 (2007) 215–223.
[5] J.C. Yu, H.Y. Tang, J. Yu, J. Photochem. Photobiol. A: Chem. 153 (2002) 211–219.
[6] A.L. Linsebigler, G. Lu, J.T. Yates Jr., Chem. Rev. 95 (1995) 735–758.
[7] A. Mills, S.L. Hunte, J. Photochem. Photobiol. A: Chem. 108 (1997) 1–35.
[8] S. Malato, J. Blanco, D.C. Alarcon, Catal. Today 122 (2007) 137–149.
[9] P.S. Mukherjee, A.K. Ray, Chem. Eng. Technol. 22 (1999) 253–260.
[10] R. Gao, A. Safrany, J. Rabani, Radiat. Phys. Chem. 65 (2002) 599–609.
[11] S. Goldstein, G. Czapski, J. Rabani, J. Phys. Chem. 98 (1994) 6586–6591.
[12] N. Chitose, S. Ueta, S. Seino, T.A. Yamamoto, Chemosphere 50 (2003) 1007–1013.
[13] Y. Du, J. Rabani, J. Phys. Chem. B 107 (2003) 11970–11978.
[14] C.S. Turchi, D.F. Ollis, J. Catal. 122 (1990) 178–192.
[15] L. Sun, J.R. Bolton, J. Phys. Chem. 100 (1996) 4127–4134.
[16] C. Wang, J. Rabani, D.W. Bahnemanna, J.K. Dohrmannb, J. Photochem. Photobiol. A: Chem. 148 (2002) 169–176.
[17] K. Ishibashi, A. Fujishima, T. Watanabe, K. Hashimoto, Electrochem. Comm. 2 (2000) 207–210.
[18] R. Morelli, I.R. Bellobono, C.M. Chiodaroli, S. Alborghetti, J. Photochem, Photobiol. A: Chem. 112 (1998) 271–276.
[19] N.Th. Rakintzis, Z. Phys. Chem. (Frankfurt am Main) 57 (1968) 99–102.
[20] J.W.T. Spinks, R.J. Woods, An Introduction to Radiation Chemistry, third ed., A Wiley-Interscience, Canada, 1990.
[21] A.J. Kettle, B.M. Clark, C.C. Winterbourn, J. Biol. Chem. 279 (2004) 18521–18525.
[22] NDRL Radiation Chemistry Data Center http://www.rcdc.nd.edu/index.html.
[23] X. Zhu, M.A. Nanny, E.C. Butler, J. Photochem. Photobiol A: Chem. 185 (2007) 289–294.
[24] M. Abdullah, G. Low, R.W. Matthews, J. Phys. Chem. 94 (1990) 6820–6825.
[25] H. Chun, Y. Tang, L. Lin, Z. Hao, Y. Wang, H. Tang, J. Chem. Technol. Biotechnol. 79 (2004) 247–252.
[26] A. Sclafani, L. Palmisano, E. Davi, J. Photochem. Photobiol. A: Chem. 56 (1991) 113–123.
[27] R.E. Huie, C.L. Clifton, P. Neta, Radiat. Phys. Chem. 38 (1991) 477–481.
[28] G.G. Jayson, B.J. Parsons, A.J. Swallow, J. Chem. Soc., Faraday Trans. 1 (69) (1973) 1597–1607.
[29] D. Zehavi, J. Rabani, J. Phys. Chem. 76 (1972) 312–319.
[30] C. Hachem, F. Bocquillon, O. Zahraa, M. Bouchy, Dyes Pigments 49 (2001) 117–125.
[31] C.G. Silva, W. Wang, J.L. Faria, J. Photochem. Photobiol. A: Chem. 181 (2006) 314–324.
[32] S. Kaur, V. Singh, J. Hazard. Mater. 141 (2007) 230–236.
[33] A. Lair, C. Ferronato, J.M. Chovelon, J.M. Herrmann, J. Photochem. Photobiol. A: Chem. 193 (2008) 193–203.
[34] H.K. Singh, M. Saquib, M.M. Haque, M. Muneer, Chem. Eng. J. 136 (2008) 77–81.
[35] V.E. Henrich, G. Dresselhaus, H.J. Zeiger, Solid State Commun. 24 (1977) 623–626.
[36] K. Tanaka, J.M. White, J. Phys. Chem. 86 (1982) 4708–4714.
[37] Y. Suda, T. Morimoto, Langmuir 3 (1987) 786–788.
[38] K. Morishige, F. Kanno, S. Ogawara, S. Sasaki, J. Phys. Chem. 89 (1985) 4404–4408.
[39] A.H. Boonstra, C.A.H.A. Mutsaers, J. Phys. Chem. 79 (1975) 1694–1698.
[40] G. Munuera, V. Rives-Arnau, A. Saucedo, J. Chem. Soc. Faraday Trans. 1 (75) (1979) 736–747.
[41] C. Doremieux-Morin, M.A. Enriquez, J. Sanz, J. Fraissard, J. Colloid Interface Sci. 95 (1983) 502–512.
[42] Y. Inel, A.N. Okte, J. Photochem. Photobiol. A: Chem. 96 (1996) 175–180.
[43] Y. Nosaka, M.A. Fox, J. Phys. Chem. 90 (1986) 6521–6522.
[44] A.J. Hoffman, E.R. Carraway, M.R. Hoffmann, Environ. Sci. Technol. 28 (1994) 776–785.
[45] L. Davydov, P.G. Smirniotis, J. Catalysis 191 (2000) 105–115.